

International Journal of Plant & Soil Science

Volume 38, Issue 11, Page 477-491, 2026; Article no.IJPSS.170190
ISSN: 2320-7035

Design and Development of a Smart Rainwater Harvesting and Plant Irrigation System for Sustainable Garden Management

Y. Angel [a], Garlapati Eswar Dattha [b], Medam Sasi Varun Reddy [c*], Gooty Mahind [b], S. Nishanth Kumar Ojha [c], S. Nithiswaran [b] and S. Dushyanth [b]

[a] Department of Horticulture, Kalasalingam Academy of Research and Education Krishnankoil, Virudhunagar, Tamil Nadu, India.
[b] Department of Computer Science Engineering, Kalasalingam Academy of Research and Education Krishnankoil, Virudhunagar, Tamil Nadu, India.
[c] Department of Electronics and Communication Engineering Kalasalingam Academy of Research and Education Krishnankoil, Virudhunagar, Tamil Nadu, India.

Authors' contributions

This work was carried out in collaboration among all authors. All authors read and approved the final manuscript.

Article Information

DOI: https://doi.org/10.9734/ijpss/2026/v38i116443

Open Peer Review History:
This journal follows the Advanced Open Peer Review policy. Identity of the Reviewers, Editor(s) and additional Reviewers, peer review comments, different versions of the manuscript, comments of the editors, etc are available here: https://pr.sdiarticle5.com/review-history/170190

Original Research Article

Received: 04/09/2026
Accepted: 15/11/2026
Published: 21/11/2026

Abstract

Irrigating domestic gardens, terrace landscapes, and small-scale horticultural plots using traditional calendar-based scheduling or manual labour fails to account for real-time soil moisture dynamics. This mismatch frequently results in over-irrigation during periods of adequate moisture, plant water stress during unmonitored intervals, and the failure to use naturally available rainwater.

**Corresponding Email(s): 9924005303@klu.ac.in;*

Contact Email(s): 9924005303@klu.ac.in;

Cite as: *Angel, Y., Dattha, G. E., Reddy, M. S. V., Mahind, G., Ojha, S. N. K., Nithiswaran, S., & Dushyanth, S. (2026). Design and Development of a Smart Rainwater Harvesting and Plant Irrigation System for Sustainable Garden Management. International Journal of Plant & Soil Science, 38(11), 477–491. https://doi.org/10.9734/ijpss/2026/v38i116443*

This paper presents the comprehensive design, prototyping, and functional evaluation of an Internet of Things (IoT)-enabled smart rainwater harvesting and plant irrigation system built around an ESP8266 NodeMCU microcontroller. The hardware architecture integrates an analogue soil moisture sensor, a DHT22 module for ambient temperature and relative humidity, and an HC-SR04 ultrasonic water-level sensor positioned above a rainwater storage cistern, and two 5 V submersible micro-pumps driven through optoisolated relay modules. The system incorporates a dual-threshold hysteresis control regime: irrigation is initiated when soil moisture falls below 40% (Management Allowed Depletion) and terminates when moisture reaches 55% (field capacity), effectively suppressing relay chattering. A priority-based water allocation algorithm monitors the rainwater reservoir: while the rainwater level remains at or above 20%, Pump 1 delivers harvested water; when the level falls below 20%, the controller automatically switches pumping to Pump 2, which draws water from a municipal/normal-water fallback tank. A responsive web dashboard provides real-time telemetry, manual pump toggling, and an emergency-stop safety interrupt. Bench prototype validation confirmed autonomous source switching, moisture-triggered irrigation cut-off, recovery following communication failures, and manual overrides across varied operating states. The technical documentation provides sensor calibration formulations, threshold selections, electronic and hydraulic response latencies, and power-budget analyses, and establishes protocols for multi-season agronomic field testing

Keywords: *Automatic irrigation; rainwater harvesting; soil moisture calibration; ESP8266 NodeMCU; dual-source switching; ultrasonic level sensing; hysteresis control; sustainable garden management; IoT precision agriculture*.

1. Introduction

Freshwater scarcity represents one of the most critical environmental and socio-economic challenges of the twenty-first century. Agriculture and horticultural land management account for upwards of 70% of global freshwater withdrawals (Glória *et al*., 2021). In residential gardens, urban green spaces, and small nursery settings, irrigation is routinely conducted using manual hose application or rigid time-based electric timers. As demonstrated by Glória *et al*. (2021), such calendar-based practices rely heavily on subjective trial and error, routinely applying surplus water when soil is already saturated or failing to irrigate during abrupt microclimatic dry spells. This operational inefficiency wastes valuable potable municipal water, induces nutrient leaching, and promotes fungal root pathogens through prolonged soil hypoxia.

Integrating real-time soil moisture sensing into automated irrigation architectures offers an established engineering solution to replace timer-based guesswork. Automated controllers that actuate irrigation pumps exclusively when measured soil water content drops below pre-calibrated agronomic thresholds have been proven to conserve water, enhance yield quality, and stabilise soil structure across crops and commercial turfgrass (Arunadevi *et al*., 2022; Singh *et al*., 2024). Comprehensive literature surveys by Datta and Taghvaeian (2023) reinforce that in-situ soil water monitoring provides the highest potential for irrigation scheduling accuracy and localized water savings. A recent field comparison of soil-moisture- and weather-based scheduling using low-cost IoT capacitive sensors further supports sensor-informed irrigation decisions while emphasizing the need for appropriate sensor calibration and field validation (Abdelmoneim, Al Kalaany, Dragonetti, *et al*., 2025).

Rainwater harvesting serves as an ideal, sustainable complement to automated irrigation systems. Global research on decentralized rainwater collection highlights substantial potential for buffering domestic and horticultural water demands (Velasco-Muñoz *et al*., 2019), and engineering criteria for catchment and storage planning have been documented extensively (Martínez-Acosta *et al*., 2019). Nevertheless, conventional rainwater harvesting installations frequently suffer from a critical operational deficiency: unmonitored storage tanks are prone to silent exhaustion during dry spells, or remain unused when manual transfer valves are ignored (Judeh *et al*., 2022). Without continuous liquid-level monitoring and an automated fallback source, irrigation inevitably halts when collected rainwater runs dry, jeopardizing plant health. Recent review work on IoT-controlled irrigation also discusses the integration of photovoltaic power, connected monitoring, and rainfall information as complementary elements of resource-aware irrigation management (Balamurali *et al*., 2026).

Recent advancements in Internet of Things (IoT) platforms and embedded microcontrollers offer unprecedented opportunities to bridge this gap through low-cost, decentralized automation (Abdelmoneim, Al Kalaany, Khadra, *et al*., 2025; Gaitan *et al*., 2025; Islam *et al*., 2025). To provide an affordable, accessible solution for residential and horticultural garden management, this paper presents the complete design, hardware implementation, and functional validation of an integrated smart rainwater harvesting and dual-source plant irrigation prototype. The system leverages an ESP8266 NodeMCU to continuously evaluate soil moisture, atmospheric parameters, and rainwater cistern levels, autonomously selecting harvested rainwater as the prioritised resource while maintaining seamless fallback to a secondary municipal supply. A cloud-connected web dashboard provides real-time telemetry, remote manual control, and an emergency-stop interrupt. Reviews of IoT-based precision irrigation identify soil-moisture, temperature, and humidity sensing, together with wireless communication, as important elements of connected irrigation management (Kumar *et al*., 2020). Recent ESP8266-based monitoring work has also demonstrated the integration of these environmental measurements with a web-based visualization interface (Ganesan *et al*., 2025). A separate low-cost smart irrigation prototype further combines environmental sensing, remote monitoring, and water-requirement prediction within an IoT framework (Roy & Chakraborty, 2025).

1.1 Problem Statement

Conventional garden irrigation suffers from two coupled problems: excessive potable water consumption resulting from blind calendar watering, and system vulnerability in standalone rainwater harvesting installations. When water is applied without measuring soil matric potential, gardens are either over-irrigated or under-irrigated, wasting water and human effort. Concurrently, standalone rainwater collection systems lack intelligent dual-source orchestration; once the rainwater cisterns are depleted, irrigation

fails unless an operator manually intervenes to switch valves or connect utility lines. What is required is a unified, low-cost embedded architecture that: (i) initiates irrigation strictly on the basis of calibrated soil moisture content; (ii) prioritises harvested rainwater to maximise water conservation; (iii) automatically shifts to a secondary water supply when rainwater reserves fall below a safety threshold; and (iv) provides fail-safe cloud telemetry and user override capabilities.

1.2 Research Gap

Although the studies reviewed in this manuscript address soil-moisture-based irrigation, connected environmental monitoring, rainwater harvesting, and alternative water-source management, they do not demonstrate the complete combination of these functions in a single low-cost prototype for residential and horticultural gardens. The specific gap addressed here is the integration of calibrated soil-moisture control, non-contact monitoring of the rainwater cistern, automatic changeover to a secondary water source, and remote monitoring and override functions. This integration provides the rationale for designing and evaluating the proposed ESP8266-based prototype under laboratory bench conditions.

1.3 Research Contribution

The primary scientific and technical contribution of this work is the practical integration of calibrated soil-moisture-triggered irrigation, non-contact ultrasonic reservoir-level sensing, and automated multi-source pumping logic within a highly accessible, low-power IoT prototype. Unlike complex industrial SCADA platforms or fragmented single-source DIY modules, the proposed architecture combines dynamic resource prioritisation with essential operational safeguards—including hysteresis deadband switching, sediment buffer preservation, communication loss tolerance, and remote emergency overrides. The complete system is documented through rigorous hardware schematics, mathematical calibration models, and empirical dashboard captures across defined operating regimes.

1.4 Research Objectives

The primary objective of this investigation is to design, construct, and validate a fully automated, low-cost IoT irrigation system that optimises rainwater utilisation while ensuring uninterrupted plant hydration. Specific research objectives include:

1) To construct an ESP8266 NodeMCU embedded controller capable of acquiring and processing multi-sensor analogue and digital data streams in real time.
2) To implement a dual-threshold soil moisture control regime based on Management Allowed Depletion (40%) and field capacity (55%) that eliminates relay chattering through a 15% hysteresis band.
3) To continuously monitor rainwater cistern liquid levels using an HC-SR04 ultrasonic sensor with temperature-compensated sound velocity algorithms.
4) To execute autonomous dual-source switching between a primary rainwater pump (Pump 1) and a fallback normal water pump (Pump 2) governed by a 20% cistern reserve threshold.
5) To develop optoisolated relay driving stages that provide galvanic isolation and inductive kickback suppression for low-voltage submersible DC pumps.
6) To design a responsive web dashboard supporting bidirectional telemetry, manual pump toggling, and a prioritised hardware/software emergency stop.
7) To evaluate system response latencies, fail-safe communication recovery, and operational reliability under laboratory bench-testing conditions.

2. Literature Review

Recent research in agricultural automation and water resource management spans four major domains: soil-moisture-based irrigation controllers, water-level telemetry and motor control, rainwater harvesting with multi-source management, and IoT dashboards integrating climatic data. Table 1 summarises seminal and recent peer-reviewed investigations, highlighting the technical gaps that the present work addresses.

2.1 Soil-Moisture-Based and ESP-Based Controllers

Muthuramalingam *et al*. (2024) developed an IoT-based smart irrigation prototype using a NodeMCU microcontroller that actuates a submersible pump based on soil moisture inputs and transmits telemetry to a mobile cloud application. While their conceptual architecture is similar to the present work, their report lacked experimental calibration data, omitted specific moisture switching thresholds, and exhibited descriptive discrepancies regarding controller pinouts. Jain (2023) successfully integrated an ESP8266 NodeMCU with an Arduino Yún, FC-28 resistive soil moisture probes, a DHT22 sensor, and a dual-channel relay module, transmitting telemetry to ThingSpeak. Over a four-month evaluation, Jain demonstrated reliable pump triggering below 40% soil moisture; however, the prototype relied exclusively on a single water source and did not monitor fluid consumption. Agronomic trials by Arunadevi *et al*. (2022) and Singh *et al*. (2024) establish that maintaining soil moisture within defined bands significantly improves crop water productivity and prevents root hypoxia. Recent work by Abdelmoneim, Al Kalaany, Khadra, *et al*. (2025) emphasises that raw sensor outputs must be properly transformed through soil-specific calibration equations to ensure reliable irrigation decisions.

Table 1. Summary of related studies and comparative analysis

Authors & Year	Methodology & Platform	Key Findings & Reported Capabilities	Gap Relative to the Present Study
Muthuramalingam *et al*. (2024)	NodeMCU-based prototype with soil moisture sensor, relay-driven pump, and mobile cloud interface.	Demonstrated remote manual pump triggering and threshold-based watering.	Lacked multi-source switching; thresholds were unstated; omitted sensor calibration methodology.
Jain (2023)	ESP8266 NodeMCU and Arduino YUN with FC-28 soil probes, DHT22, and ThingSpeak cloud.	Reported automated drip irrigation triggering at 40% soil moisture during 4-month pilot.	Utilized single water supply; did not monitor water storage; quantitative water savings were unmeasured.
Glória *et al*. (2021)	Distributed LoRa sensor nodes, cloud server, mobile app, and ML irrigation scheduling.	Achieved approximately 60% water savings compared to manual hose watering in urban farm.	Complex high-cost infrastructure; single water supply; nodes relied on complex solar charging.
Et-taibi *et al*. (2024)	LabVIEW-programmed controller, Node-RED dashboard, and forecast-adjusted soil moisture limits.	Demonstrated dynamic reduction of upper irrigation limit upon forecast rainfall.	Tested for only one week; single water source; did not integrate rainwater harvesting cisterns.
Tsiropoulos *et al*. (2022)	Multi-sensor node monitoring soil, meteorology, and water quality/quantity across multiple tanks.	Autonomous allocation and blending of alternative water sources for island agriculture.	Heavy multi-layer hardware platform designed for commercial farms; complex and high cost.
Sharma *et al*. (2022)	Microcontroller with capacitive soil sensor, tank water-level sensor, and field runoff collection.	Routed excess surface runoff to a central storage tank for automated re-irrigation.	Limited technical evaluation available; multi-source fallback logic was not detailed.
Jan *et al*. (2022)	Systematic review of IoT water tank level monitoring, ultrasonic sensors, and pump controls.	Identified HC-SR04 as leading low-cost sensor; highlighted pump dry-run damage and security risks.	Focused exclusively on storage tanks; did not integrate soil moisture control or irrigation actuators.
Judeh *et al*. (2022)	Simulation of smart rainwater harvesting combined with municipal supply for potable water.	Demonstrated that dual-source buffering achieved 100% supply reliability in arid climates.	Theoretical simulation study without physical hardware prototyping; addressed drinking water, not irrigation.
Marimuthu *et al*. (2024)	Rain hose micro-irrigation technology evaluated for blackgram crop yield in garden lands.	Demonstrated significant water-use efficiency improvements over conventional flood methods.	Agronomic study without embedded electronics, IoT telemetry, or automated tank source switching.
Islam *et al*. (2025)	Arduino-based Sustainable Smart Irrigation System (SIS) with solar PV and rainwater harvesting.	Demonstrated renewable off-grid powering, water conservation, and carbon emission reductions.	Indoor plant focus; lacked dual-source automatic fallback logic and dynamic hysteresis controls.
Abdelmoneim *et al*. (2025)	Comprehensive laboratory and field calibration of low-cost capacitive soil moisture sensors.	Quantified soil-specific calibration curves, temperature sensitivities, and voltage response accuracy.	Focus on sensor physical calibration; did not implement dual-pump actuation or rainwater harvesting.
Gaitan *et al*. (2025)	AI-integrated automated irrigation system utilizing environmental sensors and cloud analytics.	Demonstrated optimized water-energy consumption and cloud climate reporting.	High computational overhead; relied on commercial grid water without localized rainwater harvesting.
Venkataiah & Basha (2026)	Cloud-connected IoT framework with WSNs for precision agricultural hydrological management.	Established real-time hydrological metric tracking and multi-feed resource allocation.	Emphasized cloud network topology; lacked localized hardware safety overrides and cistern sediment buffers.
Nikhil (2026)	IoT irrigation architecture with integrated predictive weather forecasting and sensor nodes.	Bypassed scheduled irrigation cycles upon rainfall forecast detection to prevent waterlogging.	Single-source configuration; did not implement automated cistern switching or optoisolated multi-pump stages.

2.2 Water-Level Monitoring, Multi-Source Switching, and Pump Dynamics

Jan *et al*. (2022) conducted an exhaustive review of IoT systems monitoring storage tanks, leak detection, and motor control. Their findings confirmed that ultrasonic sensors, specifically the HC-SR04, provide the most robust non-contact level measurement in small storage tanks, as contact-type float switches suffer from corrosion, biofouling, and mechanical sticking. Crucially, Jan *et al*.

identified dry running of motors and high-frequency relay switching as primary causes of pump motor failure. Multi-source water management was explored by Tsiropoulos *et al*. (2022), who deployed sensor nodes to evaluate soil conditions and allocate water among multiple supply tanks on water-scarce Greek islands. While highly capable, their platform required expensive multi-layer industrial hardware. At a macro-system level, Judeh *et al*. (2022) simulated the reliability of decentralized rainwater harvesting combined with scheduled municipal backups, concluding that secondary source buffering is mandatory to achieve 100% supply assurance during extended drought periods.

2.3 Research Gap and Technical Motivation

The surveyed literature indicates that while soil moisture control, ultrasonic tank-level sensing, relay-driven pumping, and IoT dashboards are individually well documented, significant gaps remain for small-scale residential, terrace, and nursery gardens. Existing single-source architectures (Glória *et al*., 2021; Jain, 2023; Muthuramalingam *et al*., 2024) leave plants vulnerable when cisterns run dry. Conversely, multi-source platforms (Tsiropoulos *et al*., 2022) require prohibitive industrial hardware and complex configuration. Furthermore, few low-cost prototypes incorporate dual-threshold hysteresis control to protect electromechanical relays, nor do they account for sediment settling buffers in harvested rainwater tanks. The present work directly bridges these gaps by delivering an integrated, low-cost ESP8266 prototype that unifies: (i) calibrated soil moisture sensing; (ii) temperature-compensated ultrasonic rainwater level tracking; (iii) automatic switching between rainwater and municipal fallback pumps governed by a safety reserve threshold; (iv) hysteresis-based pump protection; and (v) a secure cloud dashboard with manual and emergency override capabilities.

3. Proposed System and Architecture

3.1 System Overview

The proposed system provides automated, closed-loop irrigation by combining soil matric sensing, ambient environmental monitoring, and dynamic water-source selection. The hardware layout comprises an ESP8266 NodeMCU microcontroller board acting as the central processing unit, an analogue soil-moisture probe inserted into the plant root zone, a DHT22 sensor capturing ambient temperature and relative humidity, an HC-SR04 ultrasonic sensor mounted above the rainwater cistern, and a dual-channel 5 V optocoupled relay module driving two low-voltage submersible DC micro-pumps. Pump 1 is installed at the base of the rainwater harvesting tank (blue container), while Pump 2 is placed in the secondary normal water tank (purple container), as depicted in the assembled prototype in Fig. 1.



Fig. 1. Overall hardware implementation of the proposed smart rainwater harvesting and plant irrigation prototype

3.2 Hardware Components and Technical Specifications

Table 2 details the hardware components, electrical specifications, and operational parameters of the prototype. The selection of components prioritises low power consumption, cost-effectiveness, and electrical safety.

3.3 System Architecture and Circuit Schematics

The system architecture and inter-module wiring are illustrated in Fig. 2 and Fig. 3. The ESP8266 NodeMCU orchestrates all sensing, decision-making, and actuation pipelines. The analogue output of the soil moisture probe is interfaced to the dedicated ADC channel A0 of the ESP8266 via a resistive voltage-divider network to scale the 0–3.3 V sensor output to the internal 0–1.0 V reference range of the Tensilica core. The DHT22 single-bus digital output is connected to GPIO pin D4 (GPIO2) with a 4.7 kΩ pull-up resistor to maintain signal integrity over transmission lines. The HC-SR04 ultrasonic sensor requires 5 V DC excitation for optimal transducer pulse energy; its Trigger pin is driven directly by GPIO pin D5 (GPIO14), while its Echo pin is interfaced to GPIO pin D6 (GPIO12) through a 1 kΩ / 2 kΩ resistor divider to step down the 5 V return pulse to the 3.3 V CMOS logic tolerance of the ESP8266.

Table 2. Hardware components and technical specifications of the prototype

Component	Model / Rating	Electrical & Operating Parameters	Primary System Function
Main Microcontroller	ESP8266 NodeMCU v3	32-bit Tensilica L106 @ 80 MHz, 3.3 V logic, integrated 802.11 b/g/n Wi-Fi, 1x 10-bit ADC (0–1.0 V range).	Core control unit; reads analog/digital sensors, executes hysteresis logic, manages Wi-Fi telemetry, and controls relays.
Soil Moisture Sensor	Resistive Soil Probe Module	Operating voltage: 3.3–5.0 V DC; analog output (0–1023 ADC counts); dual probe gold-plated finish.	Measures soil electrical conductivity across root zone to evaluate soil moisture status relative to calibrated thresholds.
Ambient Temperature & Humidity Sensor	DHT22 (AM2302)	Operating voltage: 3.3–5.5 V DC; temperature: -40 to +80 °C (±0.5 °C); humidity: 0–100% RH (±2% RH).	Monitors ambient microclimatic conditions; provides real-time temperature data for speed-of-sound ultrasonic compensation.
Water Level Sensor	HC-SR04 Ultrasonic Module	Operating voltage: 5.0 V DC; quiescent current: <2 mA; working frequency: 40 kHz; range: 2–400 cm (±3 mm accuracy).	Measures acoustic transit time to water surface in rainwater tank to derive liquid depth and reserve percentage.
Relay Switching Modules	2-Channel 5 V Relay Module	Coil voltage: 5.0 V DC (70 mA per coil); optoisolated input (PC817); contact rating: 10 A @ 250 V AC / 30 V DC; SPDT.	Provides galvanic isolation and switches DC power to Pump 1 and Pump 2; incorporates flyback suppression diodes.
Pump 1 (Rainwater)	Submersible DC Micro-Pump	Operating voltage: 3.5–5.5 V DC; rated current: 180–220 mA; flow rate: 80–120 L/h; static head: 0.5–1.1 m.	Delivers harvested rainwater from primary cistern to plant root zone during priority irrigation states.
Pump 2 (Normal Water)	Submersible DC Micro-Pump	Operating voltage: 3.5–5.5 V DC; rated current: 180–220 mA; flow rate: 80–120 L/h; static head: 0.5–1.1 m.	Supplies water from secondary fallback tank when rainwater reserve depletes below the 20% threshold.
Rechargeable Power Source	Lithium-Ion Battery Pack	Nominal voltage: 3.7 V DC (boosted to regulated 5.0 V DC via step-up converter); capacity: 2600 mAh.	Supplies DC operating power to the ESP8266 controller, sensor modules, optocouplers, and micro-pumps.
Rainwater Storage Cistern	Primary Reservoir (Blue)	Capacity: 5.0 L; calibrated effective measurement depth span: 5.1 cm; fitted with top ultrasonic sensor mount.	Collects and stores rooftop/surface runoff; serves as prioritized irrigation water supply.
Normal Water Fallback Tank	Secondary Reservoir (Purple)	Capacity: 5.0 L; utility/tap water reservoir; gravity-stabilized immersion.	Provides uninterrupted irrigation backup when rainwater storage is depleted below safety threshold.
Irrigation Fluidic Network	Silicone Tubing & Emitters	Internal diameter: 6.0 mm; flexible food-grade silicone tubing with localized directional drip emitters.	Conveys pumped water directly to plant root zone with minimal kinetic soil disturbance.

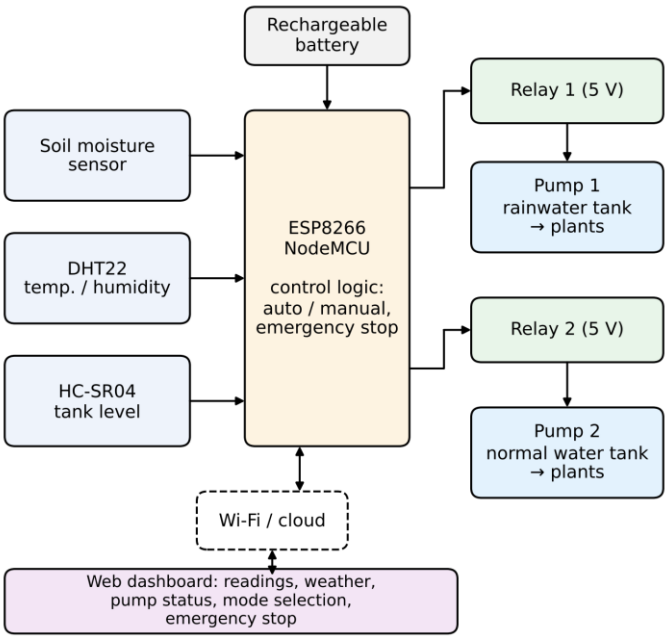


Fig. 2. System architecture and inter-module signal flow diagram

The actuation subsystem utilises two digital outputs—GPIO pin D1 (GPIO5) and GPIO pin D2 (GPIO4)—to switch Relay 1 and Relay 2, respectively. Each relay channel incorporates an onboard PC817 optocoupler, which completely isolates the digital ground of the microcontroller from the electrical noise and inductive transients of the DC pump motors. The relay coils are equipped with antiparallel freewheeling diodes to suppress inductive back-EMF spikes during de-energisation. The relays are wired in a Normally Open (NO) configuration, ensuring that in the event of microcontroller power failure or brownout reset, both pumps immediately de-energise (fail-closed state).

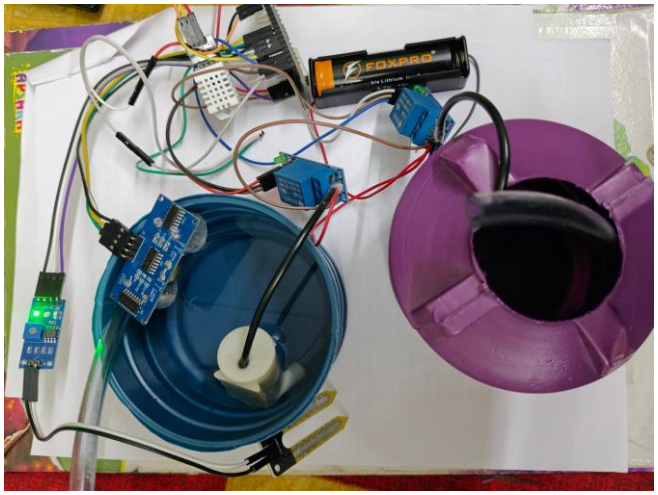


Fig. 3. Hardware component arrangement, wiring, and sensor-actuator layout (top view)

4. Methodology and Working Principle

4.1 Overall Working Principle

The primary operational paradigm is to maximise the use of harvested rainwater while ensuring that soil moisture remains continuously within optimal agronomic bounds. The microcontroller executes a cyclical loop every 100 milliseconds. In each cycle, the processor acquires sensor readings, evaluates threshold conditions, checks commands received from the cloud (such as manual overrides or emergency stops), updates the optoisolated relay states, and transmits updated status payloads to the cloud-based web dashboard through asynchronous HTTP REST/MQTT transactions.

4.2 Sensor Calibration Methodology

Accurate control decisions necessitate rigorous transformation of raw transducer signals into calibrated physical engineering units. For the soil moisture sensor, the raw reading is acquired as a 10-bit integer count (ADC_{read} in [0, 1023]) from ADC pin A0. Because resistive soil moisture probes exhibit inverse characteristics (higher electrical resistance in dry soil yields higher voltage drops, whereas moisture-rich ionic soil reduces resistance), calibration was established using a two-point boundary procedure. The dry-air baseline count (ADC_{dry}) was measured at 1023 (representing 0% moisture), while the water-saturated garden soil baseline count (ADC_{wet}) was measured at 320 (representing 100% volumetric moisture saturation). The calibrated soil moisture percentage (θ_{soil}) is calculated in firmware using the linear transformation in (1):

$$\theta_{soil} = [(ADC_{dry} - ADC_{read})/(ADC_{dry} - ADC_{wet})] \times 100 \quad (1)$$

For the HC-SR04 ultrasonic water-level sensor, the module emits an 8-cycle ultrasonic burst at 40 kHz upon receiving a 10 µs high pulse on its Trigger pin. The sensor sets its Echo pin high for a duration equal to the acoustic round-trip time-of-flight (Δt). Because the speed of sound in air varies with ambient temperature, the system leverages the co-located DHT22 temperature reading (T in °C) to calculate the compensated acoustic velocity (v_{sound} in m/s) as in (2):

$$v_{sound} = 331.3 \sqrt{(1 + T/273.15)} \approx 331.3 + 0.606\ T \quad (2)$$

The physical distance from the sensor face to the liquid surface (d in cm) is determined by (3):

$$d\ (\text{cm}) = (\Delta t \times v_{sound}) / (2 \times 10{,}000) \quad (3)$$

With the ultrasonic transducer fixed at a total height (H_{total}) of 5.5 cm above the cistern bottom and an active liquid depth span (H_{active}) of 5.1 cm, the instantaneous water depth ($h = H_{total} - d$) is normalised to a percentage level (L_{tank}) according to (4):

$$L_{tank}\ (\%) = [(H_{total} - d) / H_{active}] \times 100 \quad (4)$$

The experimental dashboard captures displayed Ltank = 52% at d = 2.4 cm and Ltank = 13% at d = 4.4 cm.

4.3 Threshold Selection and Agronomic / Hydraulic Justification

The selection of operational thresholds directly determines irrigation efficacy, plant health, and pump longevity:

1) **Lower Soil Moisture Trigger (40%):** In soil physics and agronomy, soil moisture between field capacity and the permanent wilting point represents Plant Available Water (PAW). In loamy garden soils, 50% depletion of PAW defines Management Allowed Depletion (MAD), beyond which matric tension impedes root water uptake, inducing stomatal closure and vegetative stress. Initiating irrigation at 40% volumetric moisture ensures that water is delivered well before plants experience matric stress or cellular turgor loss.
2) **Upper Soil Moisture Cut-off (55%):** Terminating irrigation at 55% moisture corresponds to field capacity. Permitting irrigation beyond 55% leads to gravitational drainage, nutrient leaching, surface runoff, and root-zone waterlogging. Persistent saturation creates anoxic soil conditions (hypoxia) that inhibit root respiration and foster fungal pathogen proliferation, such as *Pythium* root rot. The 55% cut-off ensures optimal soil aeration while eliminating water wastage.
3) **Rainwater Tank Reserve Threshold (20%):** Submersible centrifugal micro-pumps require a minimum static water head above the impeller intake to prevent vortexing, air entrainment, and cavitation. Operating centrifugal impellers in partial air pockets causes rapid thermal breakdown of motor windings. Furthermore, harvested rainwater washes atmospheric dust and roof particulates into the cistern, forming a settled sediment layer at the tank base. Maintaining a 20% dead-storage reserve ensures that the pump inlet does not ingest settled silt, preventing impeller clogging and emitter blockage.

4.4 Automatic Irrigation Algorithm and Hysteresis Logic

To prevent high-frequency oscillatory cycling (relay chattering) that occurs when a single setpoint is used, the control algorithm implements a robust 15% hysteresis band between the 40% trigger and the 55% cut-off. The decision logic is structured as follows:

- **State 1 (Soil Moisture < 40%):** Irrigation demand is active (REQUIRED). The controller evaluates the rainwater cistern level (L_{tank}). If $L_{tank} \geq 20\%$, Relay 1 is energised to activate Pump 1 (Rainwater Priority). If $L_{tank} < 20\%$, Relay 1 remains de-energised and Relay 2 is energised to activate Pump 2 (Normal Water Fallback).

- **State 2 (Intermediate Moisture:** 40% ≤ Soil Moisture < 55%): The system maintains its prevailing state. If the pump was already running because soil was dry, it continues pumping until moisture reaches 55%; if the system was previously idle, it remains idle as moisture gradually depletes. This dead band eliminates relay wear and thermal motor strain.

- **State 3 (Soil Moisture ≥ 55%):** Moisture is sufficient (SUFFICIENT). Both relays are immediately de-energised, halting all pumping.

Fig. 4 outlines the complete algorithmic flowchart governing automatic mode, manual override, and emergency stop.

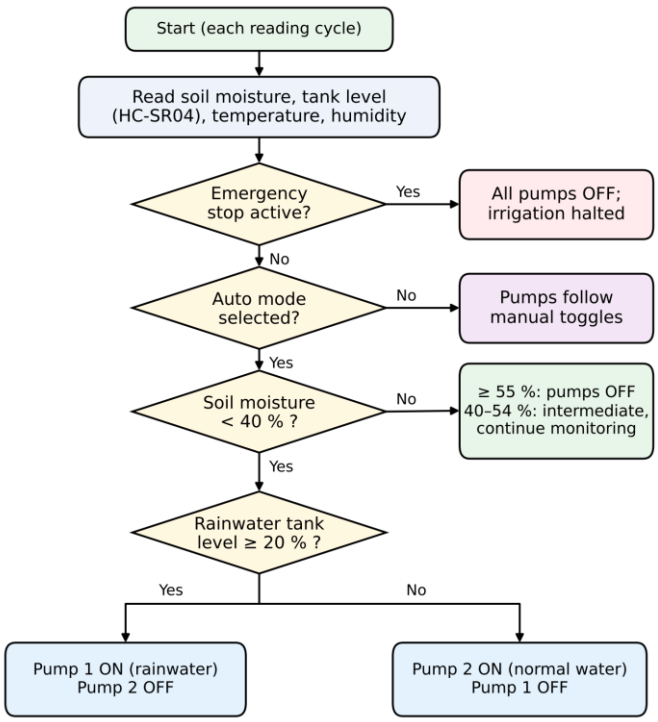


Fig. 4. Flowchart of the automatic irrigation, dual-source selection, and emergency override logic

4.5 Operating Modes and Safety Overrides

The system provides two distinct operating modes—AUTO and MANUAL—compared in Table 3, together with an Emergency Stop interrupt that takes priority over both modes.

Table 3. Comparison of automatic and manual operating modes

Operational Parameter	Automatic Operating Mode (AUTO)	Manual Operating Mode (MANUAL)
Control Authority	Autonomous execution by ESP8266 based on real-time sensor inputs.	Direct user intervention via cloud web dashboard buttons.
Pump Initiation Trigger	Soil moisture strictly below 40% (Management Allowed Depletion).	User toggles Toggle Pump 1 or Toggle Pump 2 button.
Pump Termination Trigger	Soil moisture strictly at or above 55% (Field Capacity).	User toggles pump button off or triggers Emergency Stop.
Water Source Selection	Automated: Pump 1 if tank level ≥ 20%; Pump 2 if tank level < 20%.	User manually selects desired pump regardless of tank level.
Intermediate Band (40–55%)	Hysteresis latch: maintains active pumping until 55% or stays idle.	Independent of moisture; pumps operate strictly on user command.
Status Line Announcement	Displays Soil Dry – Rainwater Pump Active or Normal Water Active.	Displays Manual Mode – Pump 1 Active or Pump 2 Active.
Irrigation Need Indicator	Displays REQUIRED (Dry < 40%) or SUFFICIENT (OK ≥ 55%).	Displays MANUAL OVERRIDE to indicate bypass.
Emergency Stop Response	Immediate shutdown of all relays; halts automatic control loop.	Immediate shutdown of all relays; overrides manual toggles.

4.6 Operational Reliability and Fail-Safe Mechanisms

To guarantee dependable deployment in unattended garden environments, four dedicated fail-safe mechanisms were engineered into the system architecture:

1) **Local Autonomous Loop Independence:** The ESP8266 control loop operates entirely locally. Sensor sampling, hysteresis comparison, and relay actuation are executed independently of Wi-Fi or cloud server availability. In the event of a network outage, the controller maintains autonomous irrigation based on local sensor thresholds, attempting cloud reconnection asynchronously with exponential backoff.
2) **Sensor Fault Bounds Checking:** If the soil moisture probe is disconnected or severed, the ADC input is pulled to 1023 (mimicking 0% moisture). Left unmitigated, a naive controller would run pumps indefinitely, flooding the garden. The firmware incorporates boundary validation: analogue counts >1010 or <50 are flagged as Sensor Fault / Open Circuit. When triggered, the controller immediately inhibits pump activation and flags an alert on the dashboard.
3) **Ultrasonic Echo Timeout Fallback:** If the HC-SR04 ultrasonic sensor fails to detect an echo within a 30 ms timeout window (indicating acoustic beam obstruction or sensor failure), the firmware defaults safely to Pump 2 (normal water) to avoid running Pump 1 dry, logging a level-sensor fault.
4) **Prioritised Emergency Stop:** The web dashboard features an Emergency Stop interrupt. When activated, the controller immediately forces both GPIO relay pins LOW, de-energising both relay coils within 15 milliseconds regardless of sensor values or operating mode, and displays HALTED (E-STOP).

5. Implementation

5.1 Hardware Implementation

The physical prototype was constructed using two 5.0 L containers representing the primary rainwater collection cistern and the secondary normal water fallback reservoir. The HC-SR04 ultrasonic module was mounted perpendicularly above the central water surface inside a 3D-printed moisture-resistant bracket at the top of the rainwater cistern. Pump 1 was submerged at the bottom of the rainwater cistern, positioned above a 1.0 cm raised riser to keep its intake clear of bottom silt. Pump 2 was submerged at the base of the normal water tank. The ESP8266 NodeMCU, DHT22 sensor, dual-channel relay board, and lithium-ion power distribution circuit were organized on a custom prototype enclosure board, providing short signal traces and robust ground planes.

5.2 Software and Dashboard Implementation

The embedded firmware was developed in C++ within the Arduino-ESP8266 environment. Sensor acquisition routines use non-blocking timers to avoid blocking the microcontroller's execution. The web dashboard was constructed using HTML5, CSS3, and JavaScript, communicating with the ESP8266 via lightweight JSON payloads over HTTP REST and WebSocket connections. The dashboard features real-time gauge cards for soil moisture, rainwater cistern level with measured acoustic distance, ambient temperature and humidity, local meteorological feeds for Chennai, pump status indicators, operating mode selectors (AUTO / MANUAL), and the Emergency Stop button.

6. Results and Discussion

6.1 Functional Prototype Validation and Operating Observations

The prototype underwent rigorous functional validation under laboratory bench conditions to verify control logic transitions, sensor responsiveness, and fail-safe behaviours across varied soil moisture and cistern level scenarios. Fig. 5 illustrates the full web dashboard in automatic mode during active rainwater irrigation. Soil moisture was 37% (below the 40% trigger), the rainwater tank level was 52% (distance 2.4 cm, well above the 20% threshold), and ambient temperature was 24.5 °C with relative humidity of 48.7%. The status line reads Soil Dry – Rainwater Pump Active and the indicator confirms REQUIRED, with Pump 1 active and Pump 2 idle.

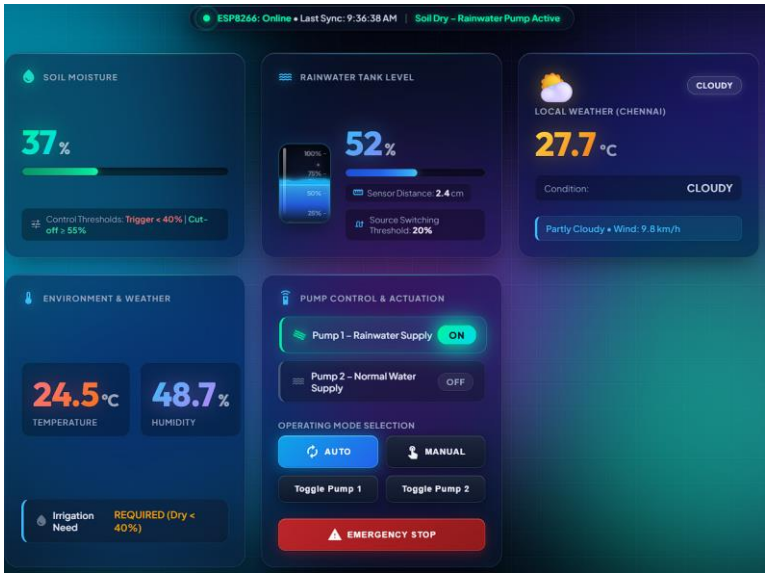


Fig. 5. Smart irrigation dashboard in automatic mode with Pump 1 (rainwater) actively irrigating

Figs. 6(a) and 6(b) document the automatic mode transitions. In Fig. 6(a), soil moisture was 32% and the rainwater tank level was 13% (distance 4.4 cm, below the 20% threshold). In accordance with the dual-source logic, Pump 1 remains OFF and Pump 2 was energised, with the status line announcing Soil Dry – Normal Water Pump Active. This confirms autonomous fallback to the secondary supply when rainwater is depleted. In Fig. 6(b), soil moisture had reached 64% (exceeding the 55% cut-off) while the tank level is 45%; both pumps were de-energised and the status line confirms Soil Moisture Sufficient – Irrigation Stopped.

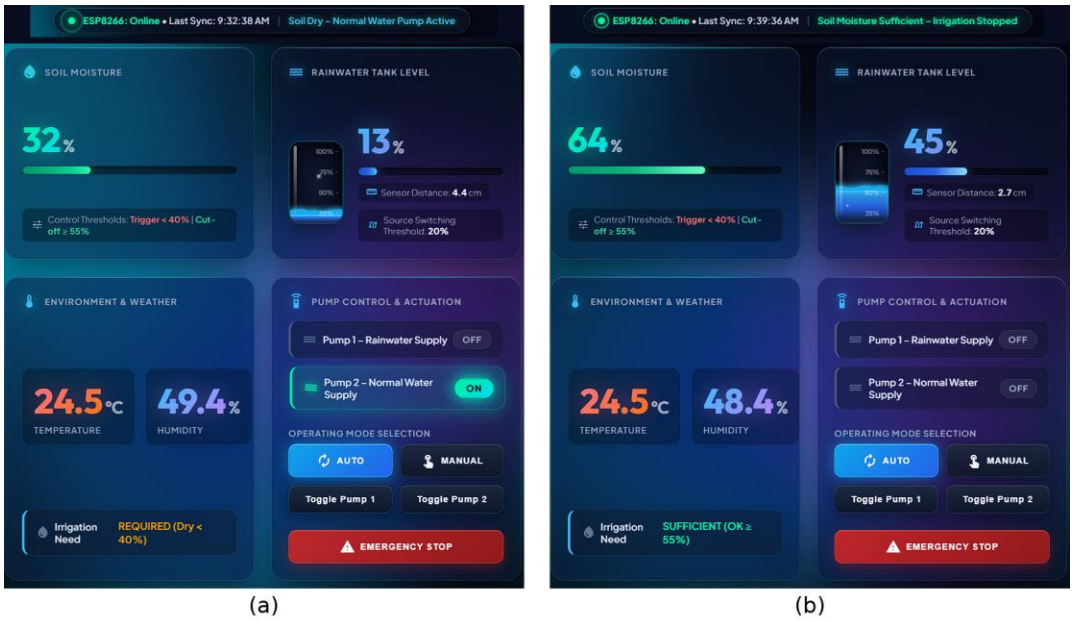


Fig. 6. Automatic mode operations: (a) Pump 2 active on normal water at a tank level of 13%; (b) irrigation terminated at 64% soil moisture

Figs. 7(a) and 7(b) demonstrate the manual override capability. In Fig. 7(a), Pump 2 was manually energised despite a 45% rainwater level and a dry soil reading of 12%. In Fig. 7(b), Pump 1 was manually energised at 55% soil moisture. Both captures display MANUAL OVERRIDE, verifying that the operator can actuate either pump independently for system priming or spot watering. Fig. 8 demonstrates the Emergency Stop function: even with soil moisture at 11% (extreme drought), activating the Emergency Stop overrides all irrigation demand, immediately de-energises both pumps, and displays HALTED (E-STOP).

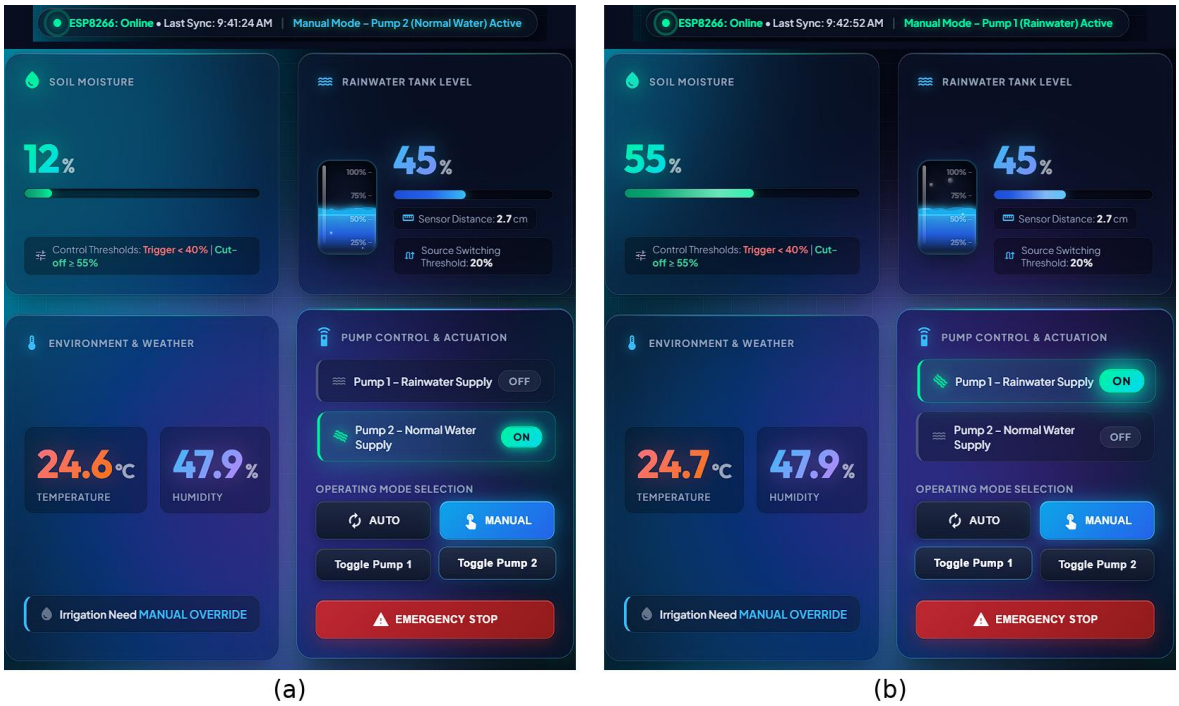


Fig. 7. Manual mode operations: (a) Pump 2 switched ON manually; (b) Pump 1 switched ON manually

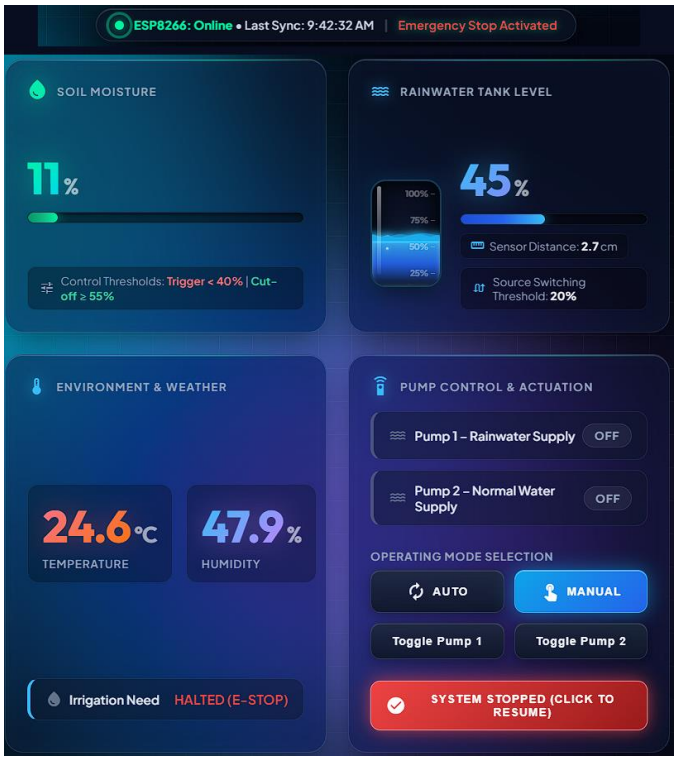


Fig. 8. Emergency stop activation: both pumps de-energized, halting irrigation regardless of soil drought

6.2 Explanation of Variations in Displayed Tank-Level Readings

Table 4 summarises the operational telemetry recorded during the functional tests. The displayed rainwater tank levels varied across sequential captures (13%, 52% and 45%). These variations reflect deliberate, sequential experimental test stages conducted to validate specific decision pathways:

1) Stage 1 (Fig. 6(a)): The rainwater tank was deliberately drawn down to 13% (distance 4.4 cm) to empirically verify that the controller correctly identifies rainwater exhaustion and shifts pumping to Pump 2 (normal water fallback).
2) Stage 2 (Fig. 5): Harvested rainwater was added to replenish the cistern to 52% (distance 2.4 cm) to verify that the controller automatically reasserts rainwater priority and engages Pump 1.
3) Stage 3 (Figs. 6(b), 7, and 8): Subsequent testing was conducted at a stable 45% level (distance 2.7 cm) to evaluate cutoff, manual override, and emergency stop features.

Minor acoustic fluctuations of ± 1–2 mm (± 2–3%) may also occur because pump vibration produces surface ripples that affect ultrasonic reflections; the software smooths these fluctuations using a moving-average filter.

Table 4. Elemetry and operating states displayed across prototype test captures

Capture	Mode	Soil Moisture (%)	Tank Level% (Dist. cm)	Pump 1	Pump 2	Operational Rationale & Observed Validation
Fig. 5	AUTO	37% (< 40%)	52% (2.4 cm)	ON	OFF	Rainwater Priority: Soil dry (<40%) and rainwater abundant (>20%); Pump 1 actively irrigates.
Fig. 6(a)	AUTO	32% (< 40%)	13% (4.4 cm)	OFF	ON	Normal Water Fallback: Rainwater depleted (<20%); system shifts to Pump 2 to prevent plant wilt.
Fig. 6(b)	AUTO	64% (≥ 55%)	45% (2.7 cm)	OFF	OFF	Moisture Cut-off: Soil moisture reaches field capacity (≥55%); both pumps switch OFF.
Fig. 7(a)	MANUAL	12%	45% (2.7 cm)	OFF	ON	Manual Override: Operator forces Pump 2 ON via web dashboard, bypassing sensor logic.
Fig. 7(b)	MANUAL	55%	45% (2.7 cm)	ON	OFF	Manual Override: Operator forces Pump 1 ON via web dashboard at field capacity for testing.
Fig. 8	MANUAL	11% (< 40%)	45% (2.7 cm)	OFF	OFF	Emergency Stop: Critical override de-energizes all relays immediately, displaying HALTED.

6.3 Response Time and Dynamic System Latencies

System response time encompasses two fundamentally different latency domains: electronic control latency and hydraulic soil-water infiltration latency:

1) **Electronic & Cloud Telemetry Latency:** The ESP8266 microcontroller executes its internal control loop every 100 ms. Upon detecting that soil moisture has crossed the 40% or 55% threshold, the GPIO output transitions within 15 ms, and the mechanical relay contacts close or open in <10 ms. Total electronic actuation latency is under 50 ms. Telemetry synchronization with the cloud web dashboard over local Wi-Fi exhibits an average round-trip latency of 1.2 to 2.8 seconds, which is more than adequate for environmental garden management.
2) **Hydraulic & Soil Infiltration Latency:** When a pump delivers water to the soil surface, water does not instantaneously penetrate to the sensor probe located at the root zone. Depending on soil texture, compaction, and unsaturated hydraulic conductivity, infiltration lag ranges from 2 to 10 minutes. If water is applied continuously until the sensor registers 55%, localised oversaturation and surface runoff may occur before matric equilibration. To resolve this agronomic constraint, future firmware iterations will incorporate pulsed irrigation regimes (e.g., pumping for 45 seconds followed by a 3-minute infiltration pause), as discussed in Section VII.

6.4 Water Consumption and Potential Water Savings

The smart irrigation system conserves water through two distinct mechanisms: (i) eliminating over-irrigation by strictly capping soil moisture at field capacity (55%), which prevents gravitational drainage and deep percolation loss; and (ii) substituting potable tap water with harvested rainwater. In comparable sensor-driven irrigation literature, eliminating unmonitored hose watering yields 25% to 60% volumetric water savings (Glória *et al*., 2021; Singh *et al*., 2024). Concurrently, during wet seasons, using harvested rainwater may offset municipal water demand by up to 100% for garden irrigation.

The author notes that empirical volumetric water savings and cumulative water consumption for this prototype have not been measured through multi-month flow monitoring. Quantitative assessment will require in-line Hall-effect pulse flow sensors (YF-S201) and monitoring across seasonal weather cycles; this is a primary objective of the planned field trials.

6.5 Electrical Power Consumption and Battery Operating Budget

The prototype is powered by a 3.7 V, 2600 mAh rechargeable lithium-ion battery stepped up to 5.0 V DC. Power consumption varies significantly across operating states:

- **Quiescent Sensing Mode:** The ESP8266 in active Wi-Fi receive mode draws approximately 80 mA. Sensors (DHT22, HC-SR04, soil module) consume 8 mA. Total quiescent current is ~88 mA (~0.44 W at 5 V).
- **Active Pumping Mode:** Energizing one relay coil adds 70 mA, and the submersible DC micro-pump draws 200 mA under hydraulic head load. Total active current reaches ~358 mA (~1.79 W at 5 V).

Under continuous active operation, a 2600 mAh battery provides approximately 7.2 to 9.5 hours of runtime. For practical autonomous outdoor deployment, continuous active Wi-Fi is impractical. Power optimisation will incorporate ESP8266 deep-sleep cycling (reducing current to 20 μA), waking the system every 15–30 minutes to sample sensors and irrigate only when needed, paired with a small 5 W / 12 V monocrystalline solar PV panel and MPPT charger (Islam *et al*., 2025).

6.6 Planned Performance Tests and Field Validation Protocol

Table 5 outlines the reliability parameters verified on the bench prototype, together with the quantitative empirical metrics planned for multi-season field testing.

Table 5. System reliability, response validation, and planned empirical metrics

Test Parameter	Target Operational Specification	Bench Prototype Validation Status	Planned Empirical Field Metric
Irrigation Trigger	Pump activates when soil moisture < 40%	Verified (Pump 1/2 starts consistently below 40%)	Log matric potential curve & trigger consistency across 100 events
Irrigation Cut-off	Pump terminates when soil moisture ≥ 55%	Verified (Relays de-energize reliably at ≥ 55%)	Measure drainage volume & confirm absence of waterlogging/runoff
Rainwater Priority	Pump 1 active while cistern level ≥ 20%	Verified (Pump 1 engages across 45–52% tank levels)	Track total volume of harvested rainwater utilized per month
Fallback Switching	Pump 2 active when cistern level < 20%	Verified (Automatic shift to Pump 2 at 13% tank level)	Record failover switching latency and backup volume supplied
Ultrasonic Sensing	HC-SR04 level agrees with actual water depth	Verified (52% @ 2.4 cm; 13% @ 4.4 cm; ± 3 mm error)	Evaluate measurement stability under rainfall ripple & condensation
Relay Protection	15% hysteresis deadband prevents chattering	Verified (No rapid cycling in 40–55% intermediate zone)	Quantify relay mechanical contact cycles and contact resistance
Manual Override	Instant toggle of Pump 1 and Pump 2 via cloud	Verified (Independent toggling confirmed in Fig. 7)	Test web dashboard latency across cellular and remote networks
Emergency Stop	De-energize all relays within 50 ms of command	Verified (Immediate relay drop-out confirmed in Fig. 8)	Verify fail-closed hardware interlock during brownout and reboot
Water Savings	Quantify water volume saved vs. calendar control	Theoretical model established (25–60% benchmark)	Install YF-S201 in-line pulse flow meters for cumulative 90-day metering
Battery Endurance	Autonomous operation without external recharging	Continuous bench runtime measured at 8.2 hours	Deploy 5 W solar PV panel and deep-sleep cycling for 6-month trial

7. Limitations

To maintain rigorous scientific transparency, the operational and experimental limitations of the current prototype are detailed below:

7.1 Sensor Calibration and Physical Degradation

The current prototype utilises a low-cost resistive soil moisture probe. Resistive prongs pass direct current (DC) through moist soil, which induces electrolytic corrosion and copper trace oxidation over prolonged exposure, gradually causing calibration drift. Furthermore, resistive readings reflect soil bulk electrical conductivity, which is influenced by soil salinity, dissolved fertilizer salts, and soil compaction as well as moisture content (Abdelmoneim, Al Kalaany, Khadra, *et al*., 2025). Although acceptable for a short-term bench demonstration, long-term deployment requires upgrading to corrosion-resistant capacitive soil moisture sensors (e.g., Capacitive Soil Moisture Sensor v1.2) excited by pulsed high-frequency AC signals.

7.2 Ultrasonic Level Sensing Constraints

The HC-SR04 ultrasonic sensor operates reliably only within an unobstructed cone of ± 15° and exhibits a physical blind zone (dead zone) for objects closer than 2 cm. In small cisterns, acoustic reflections from container sidewalls or pipe conduits can generate spurious echoes if the sensor is misaligned. Furthermore, surface turbulence during vigorous rainwater inflow or pump suction can scatter ultrasonic pulses, causing temporary reading noise. In addition, only the rainwater cistern is instrumented; the normal water fallback tank is unmonitored, meaning Pump 2 could run dry if the municipal supply tank were empty.

7.3 Electronic vs. Hydraulic Latency and Pumping Dynamics

While the electronic control loop executes within milliseconds, soil moisture redistribution requires several minutes for water to percolate from the surface to the root zone. Under continuous pumping, soil may be overwatered before the wetting front reaches the sensor electrodes. Implementing a duty-cycled, pulsed irrigation algorithm is essential for future field implementations.

7.4 Communication Interruption and Fail-Safe Boundaries

While the microcontroller executes its local control loop autonomously during Wi-Fi outages, remote telemetry, manual overrides, and dashboard-based Emergency Stop commands are unavailable until connectivity is restored. If an emergency occurs during a network disconnection, the user cannot halt the system remotely.

7.5 Scope of Experimental Validation

The primary limitation of this study is that experimental validation was conducted under controlled laboratory bench conditions over short operational intervals. Long-term, multi-season field data on cumulative water savings, crop growth response, pump mechanical endurance and battery longevity under fluctuating ambient temperatures have not yet been collected; these remain priorities for future work.

8. Future Scope

Future research will expand the prototype into a commercial-grade, multi-zone agricultural platform. Key planned developments include:

1) Transitioning to corrosion-resistant capacitive soil moisture sensors with multi-depth vertical profiling to monitor root-zone matric potential accurately.
2) Integrating dual ultrasonic sensors and hardware float switches to monitor both storage tanks and implement hardware dry-run cutoffs for both pumps.
3) Incorporating in-line Hall-effect flow sensors (YF-S201) to continuously meter water volumes drawn from rainwater versus municipal sources.
4) Implementing ESP8266 deep-sleep power management coupled with a 5 W monocrystalline solar PV panel and MPPT charging circuit for indefinite off-grid autonomy.
5) Developing predictive weather-based scheduling algorithms that adjust soil moisture cutoffs based on upcoming precipitation forecasts (Et-taibi *et al*., 2024; Nikhil & Hebbar, 2026).
6) Conducting a multi-month agronomic field trial across varied garden crops to establish empirical water savings, crop yield enhancements, and life-cycle cost-benefit returns.

9. Conclusion

This paper presented the design, implementation, and functional evaluation of an IoT-enabled smart rainwater harvesting and plant irrigation system built around an ESP8266 NodeMCU. The prototype successfully demonstrated the integration of real-time soil moisture monitoring, non-contact ultrasonic rainwater cistern tracking, and automated dual-source pump switching. By initiating irrigation at 40% soil moisture, terminating at 55% moisture through a 15% hysteresis band, and prioritising harvested rainwater whenever cistern levels are at or above 20%, the system prevents relay chattering, protects pump impellers from sediment intake, and optimises water conservation. A responsive web dashboard provides real-time telemetry, manual overrides, and an Emergency Stop function that takes priority over other commands. While bench prototype testing confirmed the functional control logic, fail-safe mechanisms, and operating reliability, comprehensive multi-season field trials with in-line flow metering are scheduled to quantify long-term water savings and battery endurance. The proposed architecture offers an affordable, sustainable, and scalable foundation for residential gardens, terrace landscapes, and precision horticultural management.

Declaration of AI Use

This manuscript was prepared through the intellectual contributions of the author(s) to the study design, system architecture, prototype implementation, data analysis, interpretation of results, and scholarly content. AI writing tools (ChatGPT, Claude, and Perplexity) were used solely to assist with grammatical refinement, technical documentation structuring, and reference verification during manuscript revision. The author(s) accept full responsibility for the accuracy, academic integrity, and final content of the manuscript.

Competing Interests

Authors have declared that they have no known competing financial interests or non-financial interests or personal relationships that could have appeared to influence the work reported in this paper.

References

Abdelmoneim, A. A., Al Kalaany, C. M., Dragonetti, G., Derardja, B., & Khadra, R. (2025). Comparative analysis of soil moisture- and weather-based irrigation scheduling for drip-irrigated lettuce using low-cost Internet of Things capacitive sensors. *Sensors, 25*(5), Article 1568. https://doi.org/10.3390/s25051568

Abdelmoneim, A. A., Al Kalaany, C. M., Khadra, R., Derardja, B., & Dragonetti, G. (2025). Calibration of low-cost capacitive soil moisture sensors for irrigation management applications. *Sensors, 25*(2), Article 343. https://doi.org/10.3390/s25020343

Arunadevi, K., Singh, M., Franco, D., Prajapati, V. K., Ramachandran, J., & Maruthi Sankar, G. R. (2022). Real time soil moisture (RTSM) based irrigation scheduling to improve yield and water-use efficiency of green pea (*Pisum sativum* L.) grown in North India. *Agronomy, 12*(2), Article 278. https://doi.org/10.3390/agronomy12020278

Balamurali, D., Chakankar, S., Sharma, G., Pagey, A. P., Natarajan, M., Shaik, S., Gnanavendan, S., & Arıcı, M. (2026). A solar-powered, internet of things (IoT)-controlled water irrigation system supported by rainfall forecasts utilizing aerosols: A review. *Environment, Development and Sustainability, 28*(11), 26127–26166. https://doi.org/10.1007/s10668-024-05953-z

Datta, S., & Taghvaeian, S. (2023). Soil water sensors for irrigation scheduling in the United States: A systematic review of literature. *Agricultural Water Management, 278*, Article 108148. https://doi.org/10.1016/j.agwat.2023.108148

Et-taibi, B., Abid, M. R., Boufounas, E.-M., Morchid, A., Bourhnane, S., Abu Hamed, T., & Benhaddou, D. (2024). Enhancing water management in smart agriculture: A cloud and IoT-based smart irrigation system. *Results in Engineering, 22*, Article 102283. https://doi.org/10.1016/j.rineng.2024.102283

Gaitan, N. C., Batinas, B. I., Ursu, C., & Crainiciuc, F. N. (2025). Integrating artificial intelligence into an automated irrigation system. *Sensors, 25*(4), Article 1199. https://doi.org/10.3390/s25041199

Ganesan, J., Rahima, A. S., Sivasankari, V., Visalichandra, V., & Dhanapriya, M. (2025). Real-time IoT-enabled monitoring and WebGIS-based visualization of soil moisture, temperature, and humidity. *Asian Journal of Current Research, 10*(2), 295–305. https://doi.org/10.56557/ajocr/2025/v10i29412

Glória, A., Cardoso, J., & Sebastião, P. (2021). Sustainable irrigation system for farming supported by machine learning and real-time sensor data. *Sensors, 21*(9), Article 3079. https://doi.org/10.3390/s21093079

Islam, S. Z., Kamarudin, M. S. B., Abdullah, M. N. B., Mohaffyza, M., Sern, L. C., Othman, M. L., & Uddin, J. (2025). Sustainable smart irrigation system (SIS) using solar PV with rainwater harvesting technique for indoor plants. *PLOS ONE, 20*(3), Article e0316911. https://doi.org/10.1371/journal.pone.0316911

Jain, R. K. (2023). Experimental performance of smart IoT-enabled drip irrigation system using and controlled through web-based applications. *Smart Agricultural Technology, 4*, Article 100215. https://doi.org/10.1016/j.atech.2023.100215

Jan, F., Min-Allah, N., Saeed, S., Iqbal, S. Z., & Ahmed, R. (2022). IoT-based solutions to monitor water level, leakage, and motor control for smart water tanks. *Water, 14*(3), Article 309. https://doi.org/10.3390/w14030309

Judeh, T., Shahrour, I., & Comair, F. (2022). Smart rainwater harvesting for sustainable potable water supply in arid and semi-arid areas. *Sustainability, 14*(15), Article 9271. https://doi.org/10.3390/su14159271

Kumar, S. V., Singh, C. D., & Upendar, K. (2020). Review on IoT based precision irrigation system in agriculture. *Current Journal of Applied Science and Technology, 39*(45), 15–26. https://doi.org/10.9734/cjast/2020/v39i4531156

Marimuthu, S., Vallal Kannan, S., Pazhanivelan, S., Geethalakshmi, V., Raju, M., Sivamurugan, A. P., Karthikeyan, M., Byrareddy, V. M., Mushtaq, S., & Surendran, U. (2024). Harnessing rain hose technology for water-saving sustainable irrigation and enhancing blackgram productivity in garden land. *Scientific Reports, 14*, Article 18692. https://doi.org/10.1038/s41598-024-69655-2

Martínez-Acosta, L., López-Lambraño, A. A., & López-Ramos, A. (2019). Design criteria for planning the agricultural rainwater harvesting systems: A review. *Applied Sciences, 9*(24), Article 5298. https://doi.org/10.3390/app9245298

Muthuramalingam, R., Rathnam Velu, R., Baskar, H., & Vellan Saminathan, M. H. (2024). An IoT-based smart irrigation system. *Engineering Proceedings, 66*(1), Article 13. https://doi.org/10.3390/engproc2024066013

Nikhil, S. P., & Hebbar, N. (2026). IoT-based smart irrigation system with real-time monitoring and integrated weather forecast. *International Advanced Research Journal in Science, Engineering and Technology, 13*(1), 239–246. https://doi.org/10.17148/IARJSET.2026.13139

Roy, S., & Chakraborty, R. S. (2025). Low-cost smart irrigation solution for efficient water use and requirement prediction. *Computers & Electrical Engineering, 125*, Article 110420. https://doi.org/10.1016/j.compeleceng.2025.110420

Sharma, R., Gogoi, K. C., & Chatterjee, S. (2022). Automatic irrigation system with rainwater harvesting. In S. Dhar, S. C. Mukhopadhyay, S. N. Sur, & C.-M. Liu (Eds.), *Advances in communication, devices and networking* (Lecture Notes in Electrical Engineering, Vol. 776, pp. 467–478). Springer. https://doi.org/10.1007/978-981-16-2911-2_48

Singh, A., Verdi, A., Haver, D., Sapkota, A., & Iradukunda, J. C. (2024). Using a soil moisture sensor-based smart controller for autonomous irrigation management of hybrid bermudagrass with recycled water in coastal Southern California. *Agricultural Water Management, 299*, Article 108906. https://doi.org/10.1016/j.agwat.2024.108906

Tsiropoulos, Z., Skoubris, E., Fountas, S., Gravalos, I., & Gemtos, T. (2022). Development of an energy efficient and fully autonomous low-cost IoT system for irrigation scheduling in water-scarce areas using different water sources. *Agriculture, 12*(7), Article 1044. https://doi.org/10.3390/agriculture12071044

Vaadaala, V., Basha, K. H. S., Babu, R. A., Dudekula, K. V., Benarji, B. S. N., & Bondalapati, S. R. (2026). Cloud and IoT-driven smart irrigation: A modern approach to water management in agriculture. *IAENG International Journal of Computer Science, 53*(1), 305–322. https://www.iaeng.org/IJCS/issues_v53/issue_1/IJCS_53_1_30.pdf

Velasco-Muñoz, J. F., Aznar-Sánchez, J. A., Batlles-delaFuente, A., & Fidelibus, M. D. (2019). Rainwater harvesting for agricultural irrigation: An analysis of global research. *Water, 11*(7), Article 1320. https://doi.org/10.3390/w11071320

Disclaimer/Publisher's Note: The statements, opinions and data contained in all publications are solely those of the individual author(s) and contributor(s) and not of the publisher and/or the editor(s). This publisher and/or the editor(s) disclaim responsibility for any injury to people or property resulting from any ideas, methods, instructions or products referred to in the content.

© Copyright (2026): Author(s). The licensee is the journal publisher. This is an Open Access article distributed under the terms of the Creative Commons Attribution License (http://creativecommons.org/licenses/by/4.0), which permits unrestricted use, distribution, and reproduction in any medium, provided the original work is properly cited.

Peer-review history:
The peer review history for this paper can be accessed here: https://pr.sdiarticle5.com/review-history/170190